Clinical Applications of Hyperpolarised Xenon-129 MRI

Editor's Pick

The editor's pick for this issue is a review article discussing the promise of hyperpolarised xenon MRI, a non-invasive imaging technique used in respiratory medicine to assess lung function, including ventilation and diffusion, without ionising radiation. By making an inert gas visible via MR spectroscopy, it allows for the visualisation and quantification of gas flow and gas exchange disruptions in the lungs. This technique has shown promise in providing reliable measurements of disease severity and assessing progression and treatment response more sensitively than conventional methods. Further multi-centre studies could help to evaluate this exciting innovation's role in different disease settings.

Authors:	*Kher Lik Ng,[1,2] James Grist,[2] Fergus Gleeson,[1,2] Emily Fraser[1] 1. Oxford University Hospitals NHS Foundation Trust, UK 2. University of Oxford, UK *Correspondence to kherlikng@nhs.net

Disclosure:	The authors have declared no conflicts of interest.
Received:	18.03.24
Accepted:	15.11.24
Keywords:	^{129}Xe, clinical applications, hyperpolarised, hyperpolarised xenon-129 (HPX), MRI, xenon.
Citation:	EMJ. 2024;9[4]:48-61. https://doi.org/10.33590/emj/UJRW1078.

Abstract

Conventional imaging modalities, the X-ray and CT, are essential diagnostic tools in respiratory medicine, providing qualitative information regarding the pattern and extent of pulmonary pathology. Neither provide information regarding the functional impact of pulmonary diseases and additional investigations are required to assess this. Hyperpolarised xenon-129 MRI (HPX-MRI) is a non-invasive, ionising-free imaging modality that can provide functional measurements of ventilation and diffusion within the lung. The MRI-based technique involves the subject breathing in an inert gas that has been hyperpolarised to make it visible using MR spectroscopy. The gas mirrors the flow of oxygen through the bronchial tree, across the alveolar membrane, and into the pulmonary capillaries, and thus disruptions in the passage of gas due to ventilation and diffusion abnormalities can be visualised and quantified. Functional measurements of ventilation and gas exchange within regional areas of the lung can be obtained. HPX-MRI has the potential to detect early lung disease not yet evident using standard investigations and has been shown to be a sensitive modality to assess treatment responses. The role of HPX-MRI in respiratory medicine has the potential to be wide-reaching, but to date it remains largely a research tool. This review article summarises the current and possible future clinical applications of HPX-MRI in the investigation and management of lung diseases, pitched at a level comprehensible and relevant to the respiratory-focused clinicians.

Key Points

1. Hyperpolarised xenon-129 MRI (HPX-MRI) is a functional imaging technique that provides global and regional measurements of ventilation and gas exchange and can assist in the assessment and management of respiratory diseases.

2. An overview of the technology and clinical applications of HPX-MRI, aimed at respiratory-focused clinicians.

3. HPX-MRI is a functional imaging modality that is safe, quantitative, and reproducible. Clinical studies have highlighted its role in phenotyping respiratory pathology, early-stage disease detection, assessing progression, and therapeutic response to treatment.

INTRODUCTION

The advent of CT has enabled the assessment of different tissue densities of internal organs in 'slices', and thereby transformed the diagnosis and management of many respiratory diseases.[1,2] Although CT provides valuable spatially resolved information about lung structure and pathology, correlating radiological findings with functional investigations is necessary to understand the physiological impact of a disease. MRI is capable of producing detailed images of soft tissue structures; however, until recently, its utility for investigating pulmonary conditions has been limited. The development of hyperpolarised gas MRI has enabled functional imaging of the airways and alveoli and provides a reliable measure of gas exchange, improving our understanding of respiratory pathology.[3,4] Hyperpolarised gas MRI can identify regional areas of abnormality and directly measure the physiological impact of disease locally and for the whole lung. This review summarises the current and potential applications of hyperpolarised xenon-129 MRI (HPX-MRI) in the investigation and management of respiratory diseases.

Conventional MRI relies on the signal generated from exciting protons to generate images. As the lung parenchyma has a high air content and low proton density, the signal generated from the lung is limited and precludes adequate structural assessment.[5] More recently, there have been some advancements in MRI resulting in enhanced visualisation of lung structure using techniques such as ultra-short echo-time and zero echo-time imaging. These approaches acquire data from the rapidly decaying signal from protons in the lungs, providing improved visualisation of structure in comparison to conventional MRI, but still does not provide visualisation of lung function.[6,7]

For many lung diseases, high-resolution CT imaging provides a diagnosis, informs the need for treatment, and enables longitudinal monitoring of disease.[8] However, traditional imaging does not assess the functional impact of diseases and may poorly differentiate incidental findings from disease in its early stage when it may be reversible or more readily treatable.[9] Current pulmonary function testing in clinical practice provides a useful 'global' assessment of lung function but lacks the ability to localise areas of lung abnormality. Given the heterogeneity of many pulmonary diseases and the way they progress, assessing regional function may provide important prognostic information. Furthermore, traditional pulmonary function testing is reliant on patient effort and technique and is associated with a degree of inherent variability (up to 15% for gas transfer), and consequently may not always provide reliable measurements.[10-12] These limitations highlight the advantage of novel and more sensitive diagnostic techniques that can both detect and assess functional components of lung disease.

Current functional imaging techniques used in clinical practice are planar ventilation/perfusion (V/Q) scintigraphy and single photon emission CT (SPECT) V/Q. These display the

distribution of radiolabelled gas and macroaggregates of albumin during the ventilation (V) and perfusion (Q) phases, respectively.[13,14] These planar images provide limited spatial information, which although improved using SPECT, has significantly lower spatial resolution than hyperpolarised gas MRI.[15,16] SPECT V/Q enables disease quantification but involves ionising radiation, limiting its use for repeated scanning in patients with chronic disease.[14,17]

The development of hyperpolarised noble gases, helium-3 (^{3}He) and xenon-129 (^{129}Xe), as inhaled contrast agents in pulmonary MRI started in the 1990s.[18-21] The inhalation of hyperpolarised xenon-129 enables direct visualisation of functioning lung structure as it flows and fills the airways and alveoli, mirroring the passage of oxygen.[22] Abnormalities in ventilation due to airway narrowing or bullae formation can be qualitatively and quantitatively measured.[15] Defects in the transfer of gas across the alveolar capillary can also be assessed, providing a sensitive measurement of the membrane and pulmonary vasculature integrity.[3]

HPX-MRI is a state-of-the-art non-invasive, ionising-radiation-free functional imaging modality that is reproducible, quantitative, safe, and involves minimal patient effort.[3,4] The potential role of this modality in respiratory medicine is wide-reaching but it remains, to date, largely a research tool. Clinical studies, however, indicate a valuable role in enhanced phenotyping, early-stage disease detection, therapeutic guidance, and improving our understanding of disease mechanisms.[23]

HYPERPOLARISED XENON-129 MRI

Conventional MRI relies upon the signal provided by protons primarily attached to water and fat molecules. Other atoms visible in an MRI scanner include the inert atmospheric gas, xenon-129, phosphorus-31, and sodium-23/carbon-13, which are present at very low natural abundance, and so detecting signals from these atoms *in vivo* is challenging.[24] However, using concentrated xenon-129 gas and a process known as 'hyperpolarisation', it is possible to transiently boost its signal by approximately 5–6 orders of magnitude for a limited time.[3,24,25] This, in turn, provides enough signal to directly image the spatial distribution and movement of inhaled xenon-129 gas *in vivo*. Hyperpolarisation is achieved when a gas mixture containing xenon-129 is fed into an optical cell containing Rubidium (Rb) vapour and a laser polarises the Rb atoms. The resulting Rb-^{129}Xe interaction transfers the electron spin polarisation to the xenon-129 nuclei.[3] This process is called spin exchange optical pumping.

To image xenon-129, a radiofrequency coil (fitted around the chest) and a broadband radiofrequency amplifier and software (for tuning to the resonance frequency of xenon-129) are required for signal detection.[4] These devices are not commonplace in most MRI units and require additional funding to purchase. The scan process involves the patient inhaling up to 1L of xenon-129 from a gas delivery bag and holding their breath for around 10–15 seconds whilst lying in the MRI scanner. Xenon-129 has been evaluated for its safety and tolerability, and major adverse effects have not been reported. Mild side effects are recognised, but are transient and include dizziness, paraesthesia, and euphoria.[26-28]

The process of hyperpolarisation therefore enables the signal from xenon-129 to be detected within the lungs after it is inhaled by the subject. Airway abnormalities causing ventilation defects, such as bronchial wall narrowing due to asthma, appear as regional signal defects and can be quantified using a gas distribution cluster-map. In this form of static ventilation imaging, measurement of ventilation deficits is represented by the ventilation defect percentage (VDP), defined as the fraction of unventilated lung. This is calculated from the ventilation defect volume divided by thoracic cavity volume, expressed as a percentage (Figure 1A).[29,30]

Delays in the diffusion of gas across the alveolar-capillary epithelium into red blood cells (RBC) due to structural abnormalities at this interface or the pulmonary vasculature,

can be quantified and assessed using 'dissolved-phase' imaging. After inhalation, xenon-129 diffuses from the alveoli (gas-phase) into the alveolar capillary membrane. About 2% of the inhaled xenon-129 then diffuses into the capillary blood stream, where it transiently binds with haemoglobin in RBCs (dissolved-phase).[3,31-33] Due to an MRI phenomenon known as 'chemical shift', xenon-129 exhibits different resonance frequencies within the three different compartments. Following detection and reconstruction of the MR data, it is possible to assess the ratio of xenon-129 within gas phase, tissue barrier and plasma (TP), and RBC components (Figures 1B and 2A).[24,34,35] Typically, 1–2% of the xenon-129 signal originates from xenon-129 dissolved in the lung tissue, and is not exclusively from xenon-129 bound to haemoglobin.

It is also possible to assess the movement of xenon-129 gas within the alveoli using 'diffusion-weighted imaging', and from this, obtain information about the integrity of the alveoli.[3] Gas movement (referred to here as 'diffusion') is mainly limited by the proximity of the surrounding tissue. Therefore, in diseases where there is destruction of the alveolar architecture (e.g. emphysema), gas can move more freely within the remaining enlarged alveolar spaces (Figure 2B). This is represented by apparent diffusion coefficient (ADC) that measures the Brownian motion of xenon-129 within the alveoli, with increased values denoting greater movement of gas due to reduced alveolar integrity.[3]

CLINICAL APPLICATIONS

Obstructive Airway Diseases Asthma

Assessment of regional ventilation defects, disease severity and treatment response

Asthma is a chronic disease characterised by airway hyper-responsiveness and inflammation, resulting in increased airways resistance.[36] The severity and distribution of the disease can be both visualised and quantified by assessing the pattern of xenon-129 within the airspaces after inhalation using ventilation maps. Typically, a heterogeneous distribution of gas is observed and ventilation defects (indicated by raised VDP) have been reported, even in cases of well-controlled asthma (Figure 1C).[29,30,37-40] Heterogeneity is normally represented by the coefficient of variation, which is calculated as the ratio of the standard deviation to the mean of the xenon-129 signal intensity. In keeping with the typically reversible nature of the disease, Svenningsen et al.[29] and Safavi et al.[37] found significant improvement in the extent of ventilation defects, alongside a reduction in the coefficient of variation on ventilation maps, following bronchodilator treatment (Figure 1C).

VDP has been found to correlate well with forced expiratory volume in 1 second (FEV_1), FEV_1/forced vital capacity (FVC) ratio, forced expiratory flow between 25% and 75% of vital capacity, fractional exhaled nitric oxide, and lung clearance index (LCI).[30,37-42] LCI is a non-imaging lung function measurement technique commonly used in children unable to undertake spirometry. LCI assesses small airway inhomogeneity by measuring the ventilation distribution of a tracer gas over cycles of tidal breathing, and has been found to be more sensitive at detecting ventilation abnormalities than FEV_1.[43,44] Following bronchodilator challenge, Safavi et al.[37] found an improvement in VDP, but not in LCI, in children with asthma, suggesting the potential capability of HPX-MRI to detect more subtle ventilation inhomogeneity than LCI and greater sensitivity in assessing response to treatment. The VDP may also provide a more accurate measure of disease severity, with Lin et al.[42] showing that higher VDP scores correlated well with clinical severity in children, assessed by number of healthcare attendances and use of corticosteroids. Given the sensitivity of HPX-MRI in identifying ventilation defects, it may also provide a more sensitive method of assessing and monitoring treatment response in comparison to conventional lung function tests (LFT). McIntosh et al.[45] and Kooner et al.[46] reviewed the impact of the novel biologic treatment,

Figure 1: Example images of hyperpolarised xenon-129 MRI.

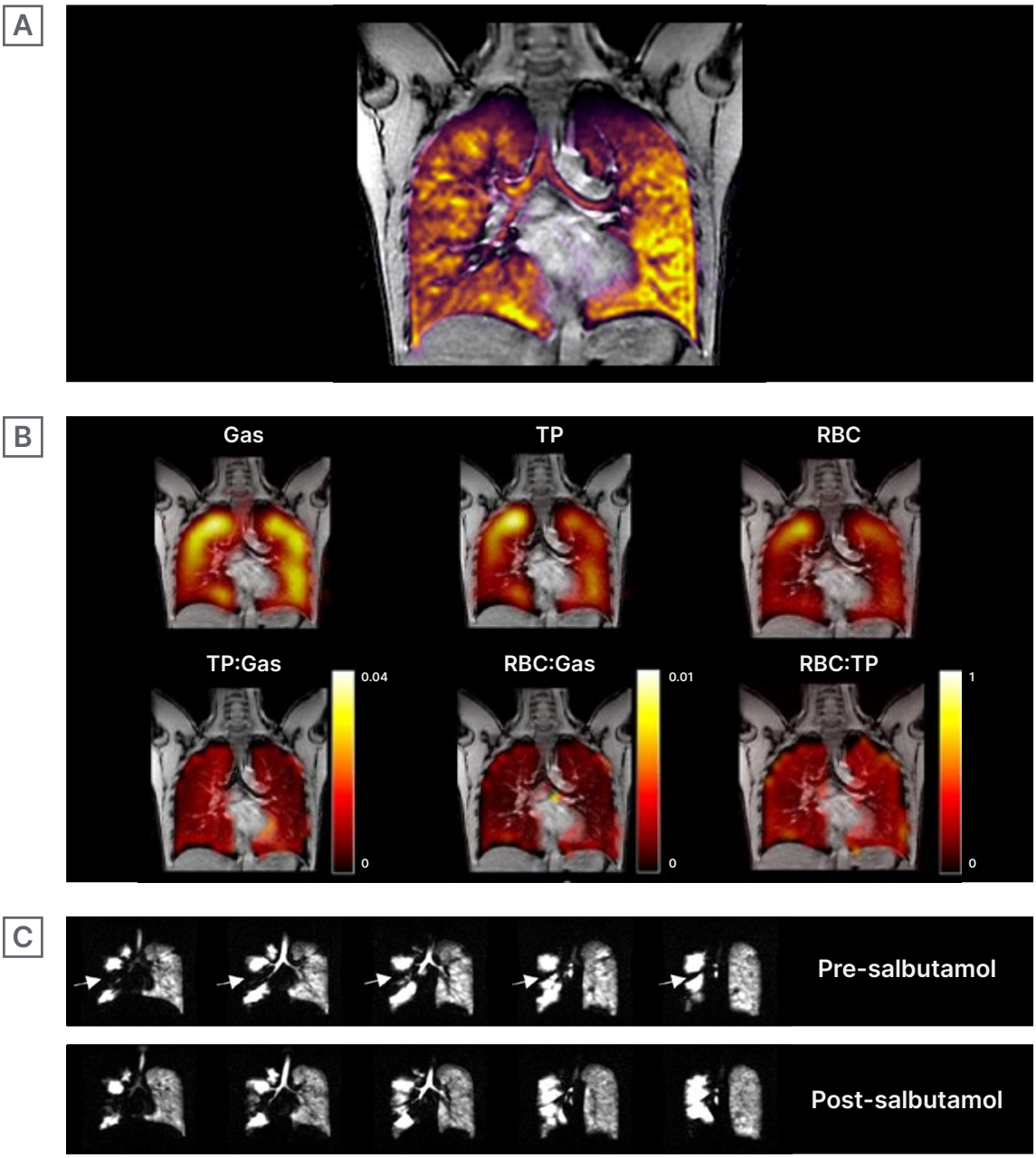

A) HPX-MRI ventilation imaging showing xenon-129 gas distribution (yellow to purple) within the tracheobronchial tree and lung fields in a young healthy control. **B)** Examples of the gas, TP, and RBC phases (not corrected for coil inhomogeneity) reconstructed into HPX-MRI ratio maps in a healthy volunteer. The gas phase demonstrated distribution of xenon-129 gas within the airways with no evidence of ventilation defects, indicative of normal airway calibre. The TP phase similarly demonstrated distribution of xenon-129 as in the gas phase, indicating normal gas transfer from the airways into the interstitial membrane and plasma. The RBC phase also demonstrated distribution of xenon-129 similar to the TP phase, demonstrating normal gas transfer into the red blood cells from the interstitial membrane and plasma. **C)** HPX-MRI ventilation images depicting ventilation defects (arrows), which improved following bronchodilator administration. There are other areas of persistent ventilation defects that had not resolved following bronchodilator administration. Original image provided by POLARIS group, University of Sheffield.

HPX-MRI: hyperpolarised xenon-129 magnetic resonance imaging; RBC: red blood cell; TP: tissue barrier and plasma.

Figure 2: Illustrative images showing the movement of xenon gas within the alveolar capillary unit.

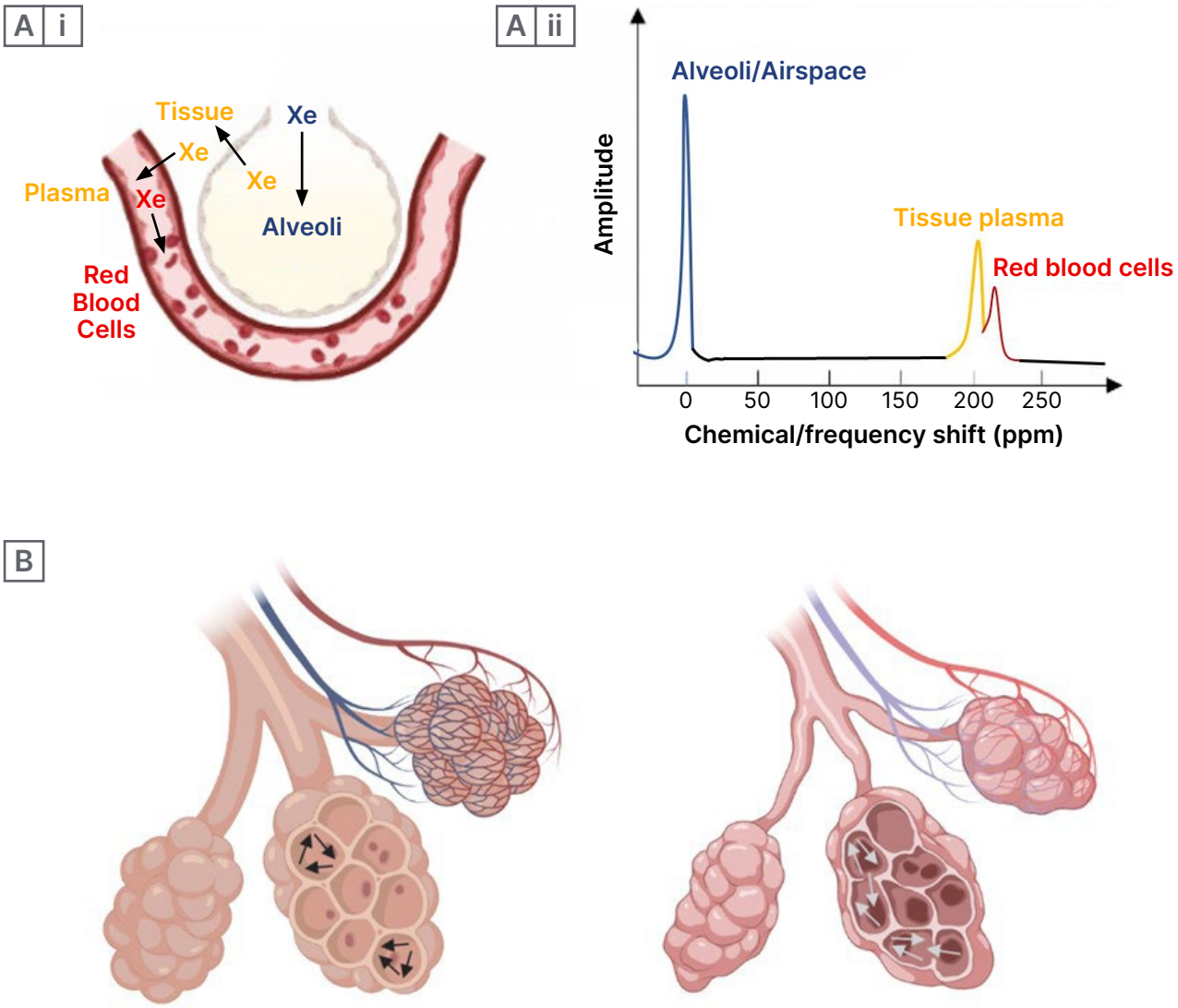

A(i) Similar to oxygen, xenon-129 moves into the alveoli during the ventilation phase, before diffusing into the tissue/alveolar membrane and plasma (blue to yellow). Xenon-129 then binds to the red blood cells (yellow to red). (Created with Biorender.com). **A(ii)** The chemical/frequency shift represents a change in the resonance frequency of xenon-129, due to alterations in the chemical environment within each compartment. When xenon-129 atoms move between compartments, the xenon-129 signal frequency changes instantaneously, occurring simultaneously with the physical movement of xenon atoms. This figure depicts the distinct frequency shifts of xenon-129 on the xenon-129 spectrum. The colour of each frequency shift in each compartment corresponds with the colour of xenon-129 in each compartment in Panel Figure A(i). **B)** Schematic description of gas flow (arrows) within the alveoli, with more free-moving gas in emphysematous alveoli due to destruction of alveolar tissue contributing to raised ADC in COPD. (Created with Biorender.com).

ADC: apparent diffusion coefficient; COPD: chronic obstructive pulmonary disease; ppm: parts per million.

benralizumab, which showed improvement in VDP, although not in FEV_1 or LCI, as early as 14-days post-treatment.

HPX-MRI also has a potential role in guiding bronchial thermoplasty. Ventilation defects have been shown to correspond to airway narrowing, and Svenningsen et al.[47] undertook HPX-MRI on patients with asthma, pre-procedure, to identify the most severely affected airways.[47] Investigators found that this image-targeted approach reduced the number of thermoplasty treatments required compared to patients enrolled in the standard non-image guided arm.[47,48]

Chronic Obstructive Pulmonary Disease

Assessment of regional ventilation defects, integrity of alveolar tissue and lung function

Chronic obstructive pulmonary disease (COPD) is characterised by persistent respiratory symptoms resulting from airflow obstruction secondary to chronic inflammation, and a variable reduction in the integrity of the lung parenchyma due to the presence of emphysema.[49] HPX-MRI can be used to quantify ventilation defects through the VDP and provide a measure of the quality of alveolar tissue via diffusion (ADC) measurements (Figure 2B and 3A). In COPD, the VDP and ADC are raised, with regional measurements typically highest in the upper lobes where emphysema is most prevalent.[50-55] The ADC correlates with measures of airflow obstruction on LFT, diffusing capacity of the lungs for carbon monoxide (DL_{co}) transfer factor, and quantitative emphysema scores on CT.[50,51,53-58] Similar to asthma, the VDP correlates well with FEV_1 and FEV_1/FVC ratio.

HPX-MRI enables the assessment of gas exchange at the alveolar-capillary membrane, providing an additional measure of functional deficit in COPD. Calculating the ratio of xenon-129 in the gas phase (i.e. within the alveoli), TP (representing the alveolar capillary membrane and plasma), and RBC from dissolved-phase imaging can provide sensitive gas transfer measurements. In COPD with emphysema, reductions are typically seen in all ratios: the TP:Gas (a measure of gas diffusion across the interstitial tissue providing information on tissue density), RBC:Gas (the HPX-MRI counterpart of DL_{CO}, and a measure of gas transfer from alveoli into the RBCs), and RBC:TP (a measure of gas exchange efficiency from interstitial tissue to blood).[55,59]

HPX-MRI may play a useful role in the early diagnosis of COPD when LFT parameters remain within normal range. Functional alveolar wall thickness can be computed from xenon-129 uptake, and has been shown to be increased in 'healthy' smokers with normal lung function compared with healthy non-smokers, thereby detecting the early-stage changes associated with COPD.[57,60-62] Using an innovative 3D alveolar gas-exchange model extrapolated from HPX-MRI dissolved-phase imaging data, the functional volume of pulmonary tissue, capillaries, and veins can be measured.[63] Unsurprisingly, this is diminished in COPD compared to healthy controls, but interestingly, significant reductions in the functional volume of pulmonary tissue were also noted in patients with only very minimal emphysematous changes on CT. This suggests a potential additional method of assessing asymptomatic early-stage disease.

A further clinical application of HPX-MRI is the potential detection of collateral ventilation in severe COPD. Collateral ventilation refers to the direct flow of air between alveolar structures, bypassing the normal airway route.[64] In severe emphysema, where lung volume reduction treatment is being considered, establishing the presence of collateral ventilation between lung lobes is essential to determining the likelihood of procedural success. Traditionally, this is assessed by two modalities: quantitative CT analysis of lung fissure integrity, and through endobronchial catheter occlusion of the lobar airway using the Chartis system® (PulmonX Inc., Redwood City, California, USA).[65] Using the Chartis system®, if there is no collateral ventilation, the occluded airway results in lobar lung collapse following the one-way expiration of air. However, in the presence of collateral ventilation, the lung lobe does not deflate

due to the flow of air from adjacent lobar structures. Whilst this method is sensitive, it is invasive, time consuming, and requires technical expertise available only in a limited number of specialist centres. Advances in dynamic HPX-MRI ventilation imaging may provide a more convenient and non-invasive alternative, enabling the measurement and visualisation of collateral ventilation in patients with COPD. This has been evaluated in studies by Marshall et al.[66,67] and Chen et al.[68] who used ^{3}He-MRI and HPX-MRI, respectively, to assess the presence of collateral ventilation, demonstrated by delayed filling of gas in non-ventilated regions (Figure 3B).

Idiopathic Pulmonary Fibrosis

Assessment of septal wall thickness, lung function, disease severity and prognosis

Idiopathic pulmonary fibrosis (IPF) is a progressive fibroproliferative disease characterised by the progressive accumulation of scar tissue that gradually replaces the normal lung parenchyma.[69] Established fibrosis is evident on CT, and disease progression is traditionally assessed through worsening CT findings and a fall in the LFT parameters, such as FVC and DL_{CO}. The role of HPX-MRI has been investigated in several research studies, and findings suggest it may be a more sensitive way of evaluating disease progression and response to treatment.

Unsurprisingly, studies using HPX-MRI dissolved-phase imaging to measure the RBC:TP and RBC:Gas have found the ratios to be consistently lower than in controls, signifying reduced gas transfer due to thickening and fibrosis of the interstitium.[70-81] These dissolved-phase parameters strongly correlated with measurements of septal wall thickness and DL_{CO}. However, RBC:TP has the advantage over DL_{CO} in that it is more reproducible (and therefore more accurate) and can directly measure the function of alveolar-capillary membrane regionally.[82] It can be measured continuously after inhalation of xenon-129, independent of the patient's effort. In IPF, the pattern of HPX-MRI abnormalities is typically most marked in the basal and peripheral lung regions, consistent with the distribution of disease.[74,78]

Studies comparing histology and CT findings have shown that early fibrotic changes identified histologically may not be evident on CT.[83,84] Through the ability of HPX-MRI to probe the lung parenchyma functionally, regional abnormalities in gas transfer can be identified that may be below the resolution of CT.[72,85] Hahn et al.[72] reported that patients with IPF who have progressive disease demonstrated a reduction in the RBC:TP in normal appearing lung, in comparison to those who did not progress over the study period.[72] Comparing visually detected and semi-quantitative assessed lung fibrosis with HPX-MRI parameters, no significant correlation was seen, suggesting that functional HPX-MRI changes may predate radiological fibrosis on CT.[77,79]

Studies evaluating HPX-MRI dissolved-phase imaging in IPF have found that the uptake of xenon-129 into the interstitial tissue (represented by TP compartment) is raised, demonstrated by an elevated TP:Gas ratio.[70,74,76,77,79,81] This indicates that there is a larger tissue volume relative to the alveolar gas volume for xenon-129 to dissolve. The apparent ratio increase can be due to fibrotic tissue formation, as well as a reduction in lung compliance, which reduces the ventilation volume and thereby increases the TP:Gas ratio. Interestingly, this finding has been identified by Qing et al.[79] even in patients with normal or mildly impaired pulmonary function tests and radiologically early disease, suggesting that HPX-MRI may pick up early fibrosis, or possibly areas of active fibrogenesis, which theoretically may have a reversible component.[79] HPX-MRI may also provide important prognostic information. Rankine et al.[80] found that the presence of both abnormal TP and RBC phases inferred an increased risk of mortality and/or the need for lung transplantation.

Long COVID/Post-COVID-19 Syndrome

Assessment of lung function

Post-COVID-19 syndrome, more commonly known as long COVID, has been defined by the National Institute for Health and Care

Figure 3: Example images of hyperpolarised helium-3 and xenon-129 MRI.

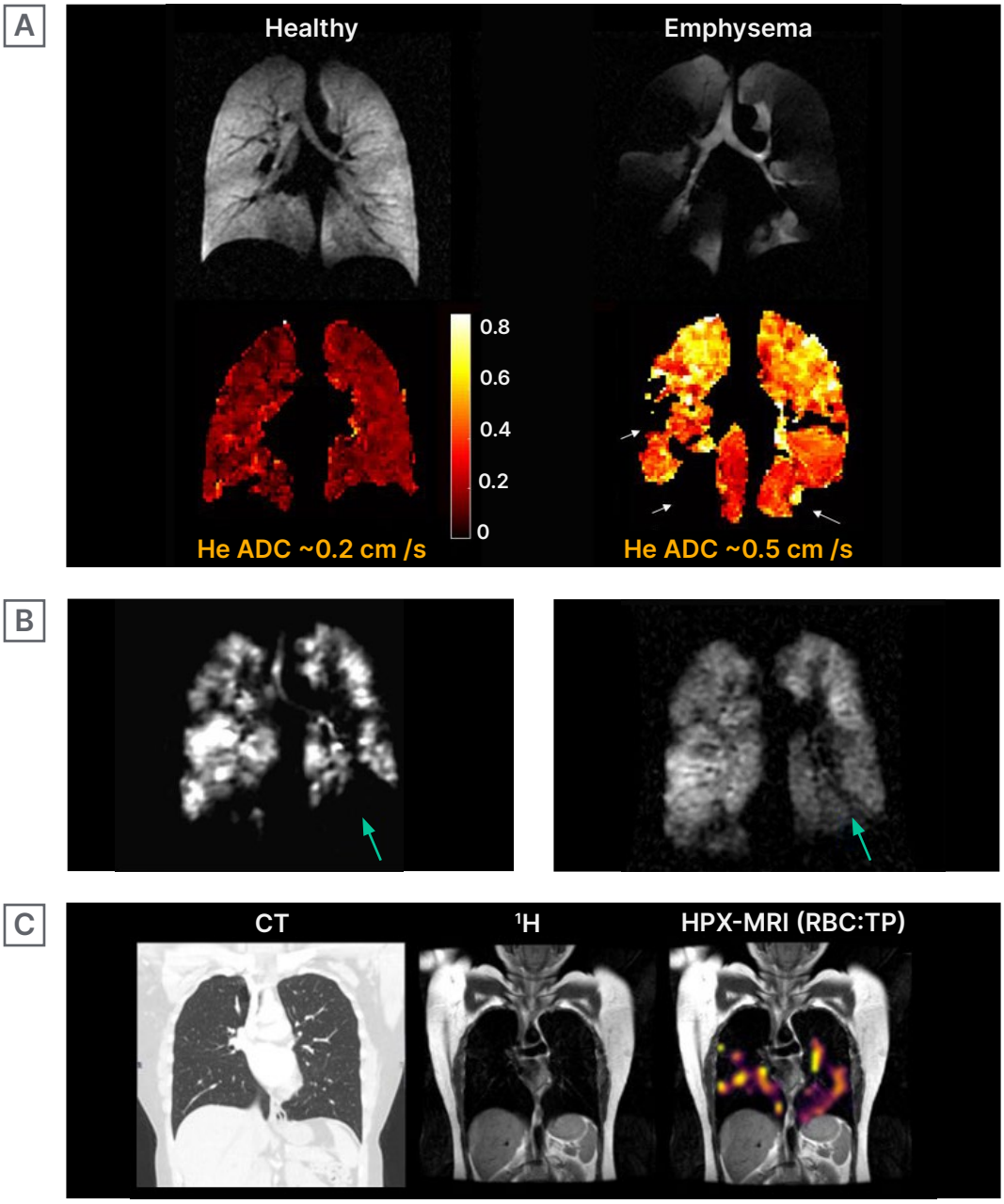

A) An example of helium-3 MRI ADC maps (HPX-MRI produces similar ADC maps) with corresponding ventilation images in a healthy volunteer and a patient with emphysematous lungs, highlighting higher ADC (bright yellow) in areas of abnormal emphysematous lungs. The patchy voids (arrows) in the ADC map of the patient with emphysematous lungs signify areas of ventilation defect where ADC cannot be quantified. The whole lung mean ADC of approximately 0.5 cm^2/s was higher in emphysematous lungs than in healthy lungs (approximately 0.2 cm^2/s). Original image provided by POLARIS group, University of Sheffield. **B)** HPX-MRI images illustrating the dynamic filling of ventilated defects (arrow) in a patient, suggesting the presence of collateral ventilation. **C)** Chest CT, proton (^1H), and RBC:TP HPX-MRI images illustrating the heterogenous pattern of xenon-129 signal and reduced RBC:TP ratio in a patient not hospitalised for COVID-19 infection with unremarkable lung parenchyma on chest CT, months after the initial infection.

ADC: apparent diffusion coefficient; HPX-MRI: hyperpolarised xenon-129 magnetic resonance imaging; RBC: red blood cell; TP: tissue barrier and plasma.

Excellence (NICE) guideline as 'signs and symptoms that develop during or following an infection consistent with COVID-19, which continue for more than 12 weeks and are not explained by an alternative diagnosis'.[86] Breathlessness is a particularly common symptom, and conventional investigations are often unremarkable.

Several studies have examined the role of HPX-MRI to investigate breathlessness in previously hospitalised patients with COVID-19. Li et al.[87] evaluated patients at baseline and at 1-month follow-up after hospital discharge with COVID-19 pneumonia and identified the presence of ventilation defects on HPX-MRI. These abnormalities were co-located within areas of residual ground glass opacification related to the primary pneumonic process. The ground glass changes on chest CT were also associated with reduced gas transfer and functional septal wall thickening, although interestingly, reduced RBC:TP ratio and raised VDP were also seen within normal areas of lung on CT. This likely indicates the persistence of microstructural damage following radiological resolution. Furthermore, Grist et al.[88] showed impaired gas transfer measured by the RBC:TP ratio in 12 patients post-COVID-19, despite a normal or near-normal chest CT 3–6 months following hospital discharge. Matheson et al.[89] reported similar findings with significantly reduced RBC:TP ratios 6–12 months after infection in 12 patients post-hospitalisation.The presence of persisting functional lung abnormalities following COVID-19 pneumonia severe enough to warrant hospitalisation is not necessarily surprising. Patients not hospitalised for COVID-19 rarely have evidence of a prior pneumonic illness on their chest CT scans, although breathlessness in this group is a common finding. Interestingly, in a small pilot study by Grist et al.[88] seven out of 11 non-hospitalised patients from the first wave of the pandemic were found to have significant reductions in RBC:TP ratio and DL_{CO} 3–15 months after their initial infection.

Although the participant numbers within these studies were small and the association with symptoms unclear, it is of note that many of the participants had their initial infection over 6 months previously, indicating that the abnormalities seen cannot be explained by a transient viral lung injury (Figure 3C).[88,89] The pathophysiology underlying these HPX-MRI abnormalities is also unknown, although, the low RBC:TP ratio suggests that the defect lies at the alveolar-capillary membrane due to either alveolar membrane damage and/or disruption of pulmonary blood flow. A larger multicentre research trial is currently underway to further assess the impact of COVID-19 on lung function using HPX-MRI.[90]

Other lung conditions

The role of HPX-MRI has also been evaluated in a range of other diseases, including cystic fibrosis (CF), lymphangioleiomyomatosis, and pulmonary hypertension (PH). In each condition, the potential main advantage of HPX-MRI over conventional investigations lies in its ability to detect early abnormalities and identify subtle changes in disease status, both in terms of treatment response and disease progression.

In CF, for example, ventilation abnormalities can be observed through VDP measurements in the absence of lung function changes.[91-104] Following antibiotics during CF exacerbation, Rayment et al.[105] found a larger improvement in the VDP than either the FEV_1 or LCI, suggesting superior sensitivity of the VDP over other measurements. In lymphangioleiomyomatosis, early cystic lung changes have been identified and can be functionally assessed through VDP and ADC measurements when spirometry values are preserved.[96,106] In the setting of PH, which is formally diagnosed via right heart catheterisation, the role of HPX-MRI has been evaluated as a non-invasive alternative.[107-109] Comparing HPX-MRI parameters to COPD, IPF, and heart failure, PH exhibited unique characteristics with focal reductions in gas transfer (RBC:TP).[107] Investigators found that in the absence of lung disease, HPX-MRI had good diagnostic accuracy when compared to right heart catheterisation in pre-capillary disease, although, further work looking at its application in a larger cohort and different subtypes of PH is

required.[108] HPX-MRI has also been studied in paediatric populations. In this setting, the modality has the advantage over conventional lung function tests due to the ease of performing the technique, as only a single breath hold is required, rather than multiple breathing manoeuvres. Furthermore, HPX-MRI measurements have been found to be highly reproducible, even between centres, making it appealing as a longitudinal tool.[101] HPX-MRI has been trialled as an alternative method to detect ventilation abnormalities in children who were unable to perform spirometry following bone marrow and stem cell transplant.[95,96,110] In bronchopulmonary dysplasia, a congenital condition characterised by diminished lung tissue due to immature alveoli formation, HPX-MRI has been utilised to quantify the extent of functional impairment through the reductions in the TP:Gas ratio.[95]

CONCLUSION

This review has summarised the versatility and potential clinical applications of HPX-MRI in the diagnosis and phenotyping of pulmonary diseases. Studies have shown that it can provide reliable measurements of disease severity, assess progression, and monitor treatment response more sensitively than conventional methods. HPX-MRI has the advantage over traditional lung function modalities by providing regional and spatial functional measurements and can detect evidence of preclinical disease. Its utility in pre-procedure assessments, such as lung volume reduction procedures, may negate the need for invasive tests. However, to date, most HPX-MRI studies have involved relatively small patient cohorts, and as a modality, it remains within the research realm. With technological advances, including improved transportability of hyper-polarised xenon-129 gas, larger multi-centre site studies are needed to further evaluate its role in different disease settings and assist in its translation into clinical practice.

References

1. Richmond C. Sir Godfrey Hounsfield. BMJ. 2004;329(7467):687.
2. Robb WL. Perspective on the first 10 years of the CT scanner industry. Academic Radiology. 2003;10(7):756-60.
3. Roos JE et al. Hyperpolarized gas MRI: technique and applications. Magn Reson Imaging Clin N Am. 2015;23(2):217-29.
4. Eddy RL, Parraga G. Pulmonary xenon-129 MRI: new opportunities to unravel enigmas in respiratory medicine. Eur Respir J. 2020;55(2):1901987.
5. Bergin CJ et al. Magnetic resonance imaging of lung parenchyma. J Thorac Imaging. 1993;8(1):12-7.
6. Hatabu H et al. Expanding applications of pulmonary MRI in the clinical evaluation of lung disorders: Fleischner Society Position Paper. Radiology. 2020;297(2):286-301.
7. Guo F et al. Ultra-short echo-time magnetic resonance imaging lung segmentation with under-annotations and domain shift. Med Image Anal. 2021;72:102107.
8. Lynch DA, Oh AS. High-spatial-resolution CT offers new opportunities for discovery in the lung. Radiology. 2020;297(2):472-3.
9. van Beek EJ, Hoffman EA. Functional imaging: CT and MRI. Clin Chest Med. 2008;29(1):195-216, vii.
10. Hruby J, Butler J. Variability of routine pulmonary function tests. Thorax. 1975;30(5):548-53.
11. Herpel LB et al. Variability of spirometry in chronic obstructive pulmonary disease. Am J Respir Crit Care Med. 2006;173(10):1106-13.
12. McCormack M. Facing the noise: addressing the endemic variability in DL_{CO} testing. Resp Care. 2012;57(1):17-25.
13. Mirza H, Hasmi MF. Lung ventilation perfusion scan (VQ scan) [Internet] (2023) Treasure Island: StatPearls. Available at: https://www.ncbi.nlm.nih.gov/books/NBK564428/. Last accessed: 17 July 2023.
14. Petersson J et al. Physiological evaluation of a new quantitative SPECT method measuring regional ventilation and perfusion. J Appl Physiol (1985). 2004;96(3):1127-36.
15. Bourhis D et al. V/Q SPECT for the assessment of regional lung function: generation of normal mean and standard deviation 3-D maps. Front Med (Lausanne). 2020;7:143.
16. Benjamin J et al. Comparison of hyperpolarized xenon-129 MR and Tc-99m DTPA aerosol lung ventilation imaging in patients with COPD and asthma. Abstract [Poster session]. Joint ISMRM-ESMRMB, 10-16 May, 2014.
17. Petersson J et al. Physiological imaging of the lung: single-photon-emission computed tomography (SPECT). J Appl Physiol (1985). 2007;102(1):468-76.
18. Ebert M et al. Nuclear magnetic resonance imaging with hyperpolarised helium-3. The Lancet. 1996;347(9011):1297-9.
19. MacFall JR et al. Human lung air spaces: potential for MR imaging with hyperpolarized He-3. Radiology. 1996;200(2):553-8.
20. Kauczor HU et al. Imaging of the lungs using 3He MRI: preliminary clinical experience in 18 patients with and without lung disease. J Magn Reson Imaging. 1997;7(3):538-43.

21. Mugler JP et al. MR imaging and spectroscopy using hyperpolarized 129Xe gas: preliminary human results. Magn Reson Med. 1997;37(6):809-15.
22. Gefter WB et al. Pulmonary functional imaging: part 2 – state-of-the-art clinical applications and opportunities for improved patient care. Radiology. 2021;299:524-38.
23. Ohno Y et al. Pulmonary functional imaging: part 1 – state-of-the-art and physiologic underpinnings. Radiology. 2021;299(3):508-23.
24. Dietrich O. Detecting COVID-19-related chronic pulmonary injury with ^{129}Xe MRI. Radiology. 2021;301(1):E373-4.
25. Beek EJR et al. Functional MRI of the lung using hyperpolarized 3-helium gas. J Magn Reson Imaging. 2004;20(4):540-54.
26. Driehuys B et al. Chronic obstructive pulmonary disease: safety and tolerability of hyperpolarized 129Xe MR imaging in healthy volunteers and patients. Radiology. 2012; 262(1):279-89.
27. Shukla Y et al. Hyperpolarized 129Xe magnetic resonance imaging: tolerability in healthy volunteers and subjects with pulmonary disease. Acad Radiol. 2012;19(8):941-51.
28. Walkup LL et al. Feasibility, tolerability and safety of pediatric hyperpolarized 129Xe magnetic resonance imaging in healthy volunteers and children with cystic fibrosis. Pediatr Radiol. 2016;46(12):1651-62.
29. Svenningsen S et al. Hyperpolarized (3) He and (129) Xe MRI: differences in asthma before bronchodilation. J Magn Reson Imaging. 2013;38(6):1521-30.
30. Ebner L et al. Hyperpolarized 129Xenon magnetic resonance imaging to quantify regional ventilation differences in mild to moderate asthma: a prospective comparison between semiautomated ventilation defect percentage calculation and pulmonary function tests. Invest Radiol. 2017;52(2):120-7.
31. Miller KW et al. Xenon NMR: chemical shifts of a general anesthetic in common solvents, proteins and membranes. Prc Natl Acad Sci USA. 1981;78(8):4946-9.
32. Swanson SD et al. Distribution and dynamics of laser-polarised ^{129}Xe magnetization in vivo. Magn Reson Med. 1999;42(6):1137-45.
33. Bifone A et al. NMR of laser-polarized xenon in human blood. Proc Natl Acad Sci USA. 1996;93(23):12932-6.
34. Marshall H et al. In vivo methods and application of xenon-129 magnetic resonance. Prog Nucl Magn Reson Spectrosc. 2021;122:42-62.
35. Mugler JP et al. Simultaneous magnetic resonance imaging of ventilation distribution and gas uptake in the human lung using hyperpolarized xenon-129. Proc Natl Acad Sci USA. 2010;107(50):21707-12.
36. British Thoracic Society and Scottish Intercollegiate Guidelines Network. British guideline on the management of asthma: a national clinical guideline. 2019. Available at: https://www.brit-thoracic.org.uk/quality-improvement/guidelines/asthma/. Last accessed: 17 July 2023.
37. Safavi S et al. Evaluating post-bronchodilator response in well-controlled paediatric severe asthma using hyperpolarised HPX-MRI: a pilot study. Respir Med. 2021;180:106368.
38. Mussell GT et al. Xenon ventilation MRI in difficult asthma: initial experience in a clinical setting. ERJ Open Res. 2021;7(3):00785-2020.
39. Svenningsen S et al. Reproducibility of hyperpolarized 129Xe MRI ventilation defect percent in severe asthma to evaluate clinical trial feasibility. Acad Radiol. 2021;28(6):817-26.
40. He M et al. Using Hyperpolarized 129Xe MRI to quantify the pulmonary ventilation distribution. Acad Radiol. 2016;23(12):1521-31.
41. Safavi S et al. Correlation of hyperpolarised Xenon-129 magnetic resonance imaging (HPX-MRI) of the lung with multi-breath washout (MBW) in children with severe asthma. Eur Res J. 2020;56:4339.
42. Lin NY et al. ^{129}Xe MRI as a measure of clinical disease severity for pediatric asthma. J Allergy Clin Immunol. 2021;147(6):2146-53.e1.
43. Davies JC et al. Lung clearance index in CF: a sensitive marker of lung disease severity. Thorax. 2008;63(2):96-7.
44. Foong RE et al. The clinical utility of lung clearance index in early cystic fibrosis lung disease is not impacted by the number of multiple-breath washout trials. ERJ Open Res. 2018;4(1):00094-2017.
45. McIntosh M et al. Response to benralizumab in severe asthma: 129Xe MRI, oscillometry and clinical measurements. Abstract D18 Asthma: Physiological Phenotypes and Treatable Traits. ATS International Conference; 15-20 May, 2020.
46. Kooner HK et al. CT mucus score predicts benralizumab response in severe asthma. Abstract TP120 Asthma: Clinical Studies. ATS International Meeting 14-19 May, 2021.
47. Svenningsen S et al. Bronchial thermoplasty guided by hyperpolarised gas magnetic resonance imaging in adults with severe asthma: a 1-year pilot randomised trial. ERJ Open Res. 2021;7(3):00268-2021.
48. Hall CS et al. Single-session bronchial thermoplasty guided by 129Xe magnetic resonance imaging. a pilot randomized controlled clinical trial. Am J Respir Crit Care Med. 2020;202(4):524-34.
49. Global Initiative for Chronic Obstructive Lung Disease. 2023 GOLD report. 2023. Available at: https://goldcopd.org/2023-gold-report-2/. Last accessed: 17 July 2023.
50. Kirby M et al. Hyperpolarized 3He and 129Xe MR imaging in healthy volunteers and patients with chronic obstructive pulmonary disease. Radiology. 2012;265(2):600-10.
51. Kaushik SS et al. Diffusion-weighted hyperpolarized 129Xe MRI in healthy volunteers and subjects with chronic obstructive pulmonary disease. Magn Reson Med. 2011;65(4): 1154-65.
52. Dregely I et al. Hyperpolarized Xenon-129 gas-exchange imaging of lung microstructure: first case studies in subjects with obstructive lung disease. J Magn Reson Imaging. 2011;33(5):1052-62.
53. Tafti S et al. Emphysema index based on hyperpolarized 3He or 129Xe diffusion mri: performance and comparison with quantitative ct and pulmonary function tests. Radiology. 2020;297(1):201-10.
54. Kirby M et al. Pulmonary ventilation visualized using hyperpolarized helium-3 and xenon-129 magnetic resonance imaging: differences in COPD and relationship to emphysema. J Appl Physiol (1985). 2013;114(6):707-15.
55. Qing K et al. Probing changes in lung physiology in COPD using CT, perfusion MRI, and hyperpolarized Xenon-129 MRI. Acad Radiol. 2019;26(3):326-34.
56. Matin TN et al. Chronic obstructive pulmonary disease: lobar analysis with hyperpolarized 129Xe MR imaging. Radiology. 2017;282(3):857-68.
57. Ruppert K et al. Using hyperpolarized Xenon-129 MRI to quantify early-stage lung disease in smokers. Acad Radiol. 2019;26(3):355-66.
58. Doganay O et al. Time-series hyperpolarized xenon-129 MRI of lobar lung ventilation of COPD in comparison to V/Q-SPECT/CT and CT. Eur Radiol. 2019;29(8):4058-67.
59. Myc L et al. Characterisation of gas exchange in COPD with dissolved-phase hyperpolarised xenon-129 MRI. Thorax. 2021;76(2):178-81.
60. Stewart NJ et al. Reproducibility of quantitative indices of lung function

and microstructure from 129 Xe chemical shift saturation recovery (CSSR) MR spectroscopy. Magn Reson Med. 2017;77(6):2107-13.

61. Kern AL et al. Mapping of regional lung microstructural parameters using hyperpolarized 129 Xe dissolved-phase MRI in healthy volunteers and patients with chronic obstructive pulmonary disease. Magn Reson Med. 2019;81(4):2360-73.
62. Kern AL et al. Regional investigation of lung function and microstructure parameters by localized 129 Xe chemical shift saturation recovery and dissolved-phase imaging: a reproducibility study. Magn Reson Med. 2019;81(1):13-24.
63. Doganay O et al. Gas exchange and ventilation imaging of healthy and COPD subjects using hyperpolarized xenon-129 MRI and a 3D alveolar gas-exchange model. Eur Radiol. 2023;33(5):3322-31.
64. Terry PB, Traystman RJ. The clinical significance of collateral ventilation. Ann Am Thorac Soc. 2016;13(12):2251-7.
65. Klooster K et al. An integrative approach of the fissure completeness score and chartis assessment in endobronchial valve treatment for emphysema. Int J Chron Obstruct Pulmon Dis. 2020;15:1325-34.
66. Marshall H et al. Direct visualisation of collateral ventilation in COPD with hyperpolarised gas MRI. Thorax. 2012;67(7):613-17.
67. Marshall H et al. Imaging collateral ventilation in patients with advanced chronic obstructive pulmonary disease: relative sensitivity of 3 He and 129 Xe MRI. J Magn Reson Imaging. 2019;49(4):1195-7.
68. Chen M et al. Delayed ventilation assessment using fast dynamic hyperpolarised Xenon-129 magnetic resonance imaging. Eur Radiol. 2020;30(2):1145-55.
69. National Institute for Health and Care Excellence (NICE). Idiopathic pulmonary fibrosis in adults: diagnosis and management. 2017. Available at: https://www.nice.org.uk/guidance/cg163/resources/idiopathic-pulmonary-fibrosis-in-adults-diagnosis-and-management-pdf-35109690087877. Last accessed: 17 July 2023.
70. Kaushik SS et al. Measuring diffusion limitation with a perfusion-limited gas--hyperpolarized 129Xe gas-transfer spectroscopy in patients with idiopathic pulmonary fibrosis. J Appl Physiol (1985). 2014;117(6):577-85.
71. Stewart NJ et al. Experimental validation of the hyperpolarized 129 Xe chemical shift saturation recovery technique in healthy volunteers and subjects with interstitial lung disease. Magn Reson Med. 2015;74(1):196-207.
72. Hahn AD et al. Hyperpolarized 129Xe MR spectroscopy in the lung shows 1-year reduced function in idiopathic pulmonary fibrosis. Radiology. 2022;305(3):688-96.
73. Weatherley ND et al. Hyperpolarised xenon magnetic resonance spectroscopy for the longitudinal assessment of changes in gas diffusion in IPF. Thorax. 2019;74(5):500-2.
74. Mummy DG et al. Hyperpolarized 129Xe MRI and spectroscopy of gas-exchange abnormalities in nonspecific interstitial pneumonia. Radiology. 2021;301(1):211-20.
75. Robertson SH et al. Uncovering a third dissolved-phase 129 Xe resonance in the human lung: quantifying spectroscopic features in healthy subjects and patients with idiopathic pulmonary fibrosis. Magn Reson Med. 2017;78(4):1306-15.
76. Wang Z et al. Quantitative analysis of hyperpolarized 129 Xe gas transfer MRI. Med Phys. 2017;44(6):2415-28.
77. Wang JM et al. Using hyperpolarized 129Xe MRI to quantify regional gas transfer in idiopathic pulmonary fibrosis. Thorax. 2018;73(1):21-8.
78. Collier GJ et al. Dissolved 129 Xe lung MRI with four-echo 3D radial spectroscopic imaging: quantification of regional gas transfer in idiopathic pulmonary fibrosis. Magn Reson Med. 2021;85(5):2622-33.
79. Qing K et al. Hyperpolarized Xenon-129: a new tool to assess pulmonary physiology in patients with pulmonary fibrosis. Biomedicines. 2023;11(6):1533.
80. Rankine LJ et al. 129Xenon gas exchange magnetic resonance imaging as a potential prognostic marker for progression of idiopathic pulmonary fibrosis. Ann Am Thorac Soc. 2020;17(1):121-5.
81. Mata J et al. Evaluation of regional lung function in pulmonary fibrosis with Xenon-129 MRI. Tomography. 2021;7(3):452-65.
82. Mammarappallil JG et al. New developments in imaging idiopathic pulmonary fibrosis with hyperpolarized Xenon magnetic resonance imaging. J Thorac Imaging. 2019;34(2):136-50.
83. Schettino IA et al. Accuracy of high resolution CT in assessing idiopathic pulmonary fibrosis histology by objective morphometric index. Pathol Res Pract. 2002;198(5):347-54.
84. Yagihashi K et al. Radiologic-pathologic discordance in biopsy-proven usual interstitial pneumonia. Eur Respir J. 2016;47(4):1189-97.
85. Kaushik SS et al. Single-breath clinical imaging of hyperpolarized (129)Xe in the airspaces, barrier, and red blood cells using an interleaved 3D radial 1-point Dixon acquisition. Magn Reson Med. 2016;75(4):1434-43.
86. National Institute for Health and Care Excellence (NICE). NICE, SIGN and RCGP set out further details about the UK guideline on management of the long-term effects of COVID-19. 2020. Available at: https://www.nice.org.uk/news/article/nice-sign-and-rcgp-set-out-further-details-about-the-uk-guideline-on-management-of-the-long-term-effects-of-covid-19. Last accessed: 20 April 2023.
87. Li H et al. Damaged lung gas exchange function of discharged COVID-19 patients detected by hyperpolarized 129Xe MRI. Sci Adv. 2021;7(1):eabc8180.
88. Grist JT et al. Lung abnormalities depicted with hyperpolarized Xenon MRI in patients with long COVID. Radiology. 2022;305(3):709-17.
89. Matheson AM et al. Persistent (129) Xe MRI pulmonary and CT vascular abnormalities in symptomatic individuals with post-acute COVID-19 syndrome. Radiology. 2022;305(2):466-76.
90. University of Oxford. An investigation to explore the use of a type of MRI scan using an inhaled gas in identifying lung damage associated with long COVID sufferers. ISRCTN14304264. 2022. Available at: https://www.isrctn.com/ISRCTN14304264. Last accessed: 24 November 2024.
91. Alam FS et al. Intra- and inter-visit repeatability of 129 xenon multiple-breath washout MRI in children with stable cystic fibrosis lung disease. J Magn Reson Imaging. 2023;58(3):936-48.
92. Couch MJ et al. A two-center analysis of hyperpolarized 129Xe lung MRI in stable pediatric cystic fibrosis: potential as a biomarker for multi-site trials. J Cyst Fibros. 2019;18(5): 728-33.
93. Kaireit TF et al. flow volume loop and regional ventilation assessment using phase-resolved functional lung (PREFUL) MRI: comparison with 129 Xenon ventilation MRI and lung function testing. J Magn Reson Imaging. 2021;53(4):1092-105.
94. Shammi UA et al. Comparison of hyperpolarized 3He and 129Xe MR imaging in cystic fibrosis patients. Acad Radiol. 2022;29 (Suppl 2):S82-90.
95. Willmering MM et al. Pediatric 129 Xe gas-transfer MRI-feasibility and applicability. J Magn Reson Imaging. 2022;56(4):1207-19.

96. Roach DJ et al. Hyperpolarized 129Xenon MRI ventilation defect quantification via thresholding and linear binning in multiple pulmonary diseases. Acad Radiol. 2022;29 Suppl 2(Suppl 2):S145-55.

97. Couch MJ et al. Comparison of functional free-breathing pulmonary 1H and hyperpolarized 129Xe magnetic resonance imaging in pediatric cystic fibrosis. Acad Radiol. 2021;28(8):e209-18.

98. Thomen RP et al. Hyperpolarized 129Xe for investigation of mild cystic fibrosis lung disease in pediatric patients. J Cyst Fibros. 2017;16(2):275-82.

99. Kanhere N et al. Correlation of lung clearance index with hyperpolarized 129Xe magnetic resonance imaging in pediatric subjects with cystic fibrosis. Am J Respir Crit Care Med. 2017;196(8):1073-5.

100. Zanette B et al. A 3D stack-of-spirals approach for rapid hyperpolarized 129 Xe ventilation mapping in pediatric cystic fibrosis lung disease. Magn Reson Med. 2023;89(3):1083-91.

101. Marshall H et al. 129 Xe and free-breathing 1 H ventilation MRI in patients with cystic fibrosis: a dual-center study. J Magn Reson Imaging. 2023;57(6):1908-21.

102. Thomen RP et al. Regional Structure-Function in Cystic Fibrosis Lung Disease Using Hyperpolarized 129Xe and ultrashort echo magnetic resonance imaging. Am J Respir Crit Care Med. 2020;202(2):290-2.

103. Willmering MM et al. Sensitive structural and functional measurements and 1-year pulmonary outcomes in pediatric cystic fibrosis. J Cyst Fibros. 2021;20(3):533-9.

104. Smith LJ et al. The assessment of short and long term changes in lung function in CF using 129Xe MRI. Eur Respir J. 2020;56(6):2000441.

105. Rayment JH et al. Hyperpolarised 129Xe magnetic resonance imaging to monitor treatment response in children with cystic fibrosis. Eur Respir J. 2019;53(5):1802188.

106. Walkup LL et al. Cyst ventilation heterogeneity and alveolar airspace dilation as early disease markers in lymphangioleiomyomatosis. Ann Am Thorac Soc. 2019;16(8):1008-16.

107. Dahhan T et al. Abnormalities in hyperpolarized (129)Xe magnetic resonance imaging and spectroscopy in two patients with pulmonary vascular disease. Pulm Circ. 2016;6(1):126-31.

108. Bier EA et al. Noninvasive diagnosis of pulmonary hypertension with hyperpolarised 129Xe magnetic resonance imaging and spectroscopy. ERJ Open Res. 2022;8(2):00035-2022.

109. Wang Z et al. Diverse cardiopulmonary diseases are associated with distinct xenon magnetic resonance imaging signatures. Eur Respir J. 2019;54(6):1900831.

110. Walkup LL et al. Xenon-129 MRI detects ventilation deficits in paediatric stem cell transplant patients unable to perform spirometry. Eur Respir J. 2019;53(5):1801779.